Performance of a Torsional Thrust Stand with 1 μN Sensitivity

IEPC-2015-261／ISTS-2015-b-261

Presented at Joint Conference of 30th International Symposium on Space Technology and Science 34th International Electric Propulsion Conference and 6th Nano-satellite Symposium, Hyogo-Kobe, Japan July 4 – 10, 2015

Andrea G. Hsu Schouten[1], Edward J. Beiting[2], and Thomas J. Curtiss[3]
The Aerospace Corporation, El Segundo, CA, 90245, USA

Abstract: The performance of a torsional thrust stand with 1 μN sensitivity is presented. In this implementation, a micro-thruster is balanced on a rotating arm whose motion is impeded by a flexure pivot (Figure 1). The thrust is calculated from the rotation of the arm using an optical displacement meter in an open-loop configuration. In situ calibration to a maximum force of 100 μN was made using the electrostatic force exerted between a pair of electrodes mounted to the thrust stand arm. The calibration was verified by measurements of the electrostatic force on a benchtop balance with a resolution of better than 0.3 μN. The results are shown in Figure 2. The flexure pivot spring constant was measured experimentally. The thrust stand is best suited for steady-state thrust measurements, and has a resolution of better than +/-1 μN limited primarily by chamber pump vibrations. Discussions of the calibration procedure, measurement resolution, and sources of uncertainties (noise) are included. The thrust stand was used to measure performance of an ion electrospray thruster inside of a vacuum chamber at pressures of 1 to 3 x 10^{-6} torr.

Nomenclature

T	=	thrust (Newtons)
θ	=	thrust stand arm deflection (radians)
k	=	spring constant (N*m/rad)
L	=	moment arm (m)
F	=	force (Newtons)
V	=	voltage (V)
A	=	surface area (m^2)
D	=	electrode separation (m)

[1] Propulsion Science Department, Andrea.G.Hsu@aero.org
[2] Propulsion Science Department, Edward.J.Beiting@aero.org
[3] Propulsion Science Department, Thomas.J.Curtiss@aero.org

I. Introduction

MICROPROPULSION is important to the spacecraft community because it enables small satellites (i.e. CubeSats) to accomplish missions such as orbital transfers, formation flight, station keeping, and attitude control not previously possible given the large power consumption of most spacecraft propulsion systems. In particular, scalable technologies that are transferable from CubeSat testbeds to larger (i.e. normal-sized) satellites are particularly interesting for two reasons. First, CubeSats can provide inexpensive, rapid TRL advancement, quickly space-qualifying the technology. Second, directly scalable technologies inherently provide redundancy on larger satellite systems. Currently, there are a number of candidate micropropulsion technologies in various TRL stages, the most common of which in the literature include colloidal microthrusters, pulsed plasma thrusters, field-emission electric propulsion thrusters, ion electrospray thrusters.

Characterization of such thrusters require thrust stands that can measure μN thrust levels, as there are currently no vacuum-compatible load cells that are capable of these measurements. The majority of μN thrust stands are of a torsional-type design and may be used to measure either steady-state or impulse thrust. A torsional-type thrust stand is based on the idea that a rigid arm is either balanced atop a flexure pivot, or hung from a torsional thread/fiber. The thruster is located on one end of the moment arm, and balanced on the opposite side by counterweights. When the thruster fires, a force is exerted on the thrust stand causing the arm to rotate about its center of gravity. By knowing the fiber/flexure pivot's spring constant, the thrust can be directly calculated. Many torsional thrust stands have been documented in the literature.[1-5] These torsional thrust stands vary in both their operation and calibration procedures. In operation, the thrust stand may be either closed-loop or open-loop. In closed-loop operation, the thrust stand is stabilized by an electrostatic actuator and not allowed to rotate. The force applied by the actuator is measured and used to calculate the force exerted by the thruster. In open-loop operation, the thrust stand is free to rotate, and the displacement is directly measured. The most common calibration methods include orifice (cold-gas) thrusters and electrostatic forces. The thrust stand described in this paper is an open-loop, flexure pivot design utilizing electrostatic calibration.

II. Thrust Stand Working Principle and Design

The thrust stand is based on a torsional design and consists of a rigid aluminum arm, balanced atop a frictionless pivot with a calibrated spring constant. Similar designs have been documented in the literature.[3,6,7] The thruster is mounted on one side of the arm, and counterweights are used to balance the arm on the opposite side. When the thruster fires, the arm is displaced, and the displacement is measured via an optical displacement meter; the thrust is calculated directly from the resulting displacement and the known spring constant. The instrument is highly sensitive, able to pick up such movements as the footsteps of passerby scientists, pump-generated noise, and even earthquake activity. A simplified schematic is shown in Fig. 1, above a photo of the experimental setup.

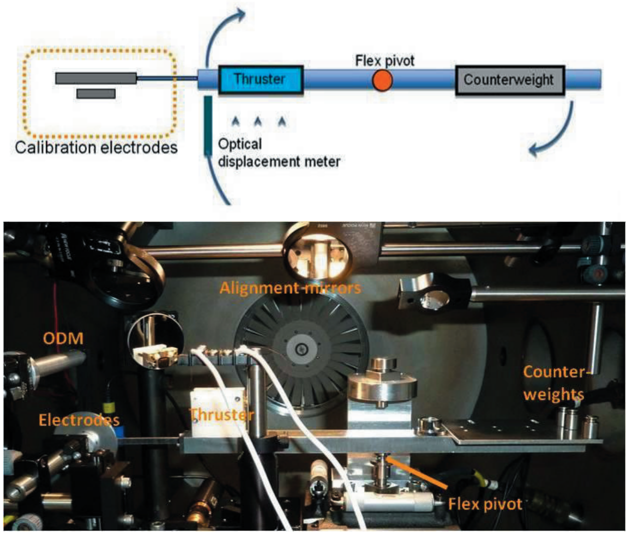

Figure 1. Simplified schematic of the thrust stand (top) and photo of the experimental setup (bottom)

The main arm of the thrust stand is made of rectangular aluminum tubing to save weight while maximizing rigidity. The pivot spring constant is nominally 0.0279 in*lb/deg (Riverhawk Industries) and is held in place by custom stainless steel mounts. The flex pivot has an axial load limit of 38 lbs. The thrust stand is calibrated using known electrostatic forces between a pair of bare aluminum electrodes, shown on the left side of the thrust stand. The electrodes are held far from the thrust stand body to minimize fringing effects. A delrin flag attached to the back of the larger electrode which holds a small (7 mm diameter) mirror and is the target for the optical displacement meter (Philtec). The moment arms for the electrodes and the optical displacement meter are equivalent (23 cm), and the moment arm to the thruster is 12.7 cm.

A. Working Principle

Thrust in a torsional-type thrust stand is calculated directly from Eq. (1):

$$T = \frac{\theta * k}{L} \tag{1}$$

Where T is thrust (Newtons), θ is the deflection of the arm (radians), k is the spring constant (N*m/rad), and L is the moment arm (m). In this case, θ is directly measured via the optical displacement meter. The spring constant is estimated by the manufacturer, but the exact value was measured. To experimentally measure k, calibration electrodes were utilized to exert a known electrostatic force on the thrust stand. The calibration electrodes were made of bare aluminum and had 0.75" and 2" diameters. The 0.75" electrode was mounted to a translational stage and the 2" electrode was mounted to the thrust stand. One electrode has a larger diameter than the other to minimize fringing effects. Given a known bias between the electrodes, the force could be calculated from Eq. (2) for a parallel-plate capacitor:

$$F = \frac{1}{2}\varepsilon_0 \left(\frac{V}{D}\right)^2 A \tag{2}$$

Where F is force (Newtons), V is the voltage difference, D is the electrode separation, and A is the surface area, in this case, of the smaller electrode. However, the force was experimentally measured using a microbalance (and compared to the calculated value) for increased measurement accuracy.

B. Design considerations

Two main experimental factors affect the accuracy and precision of the thrust stand during a measurement. The first is the leveling (i.e. balancing) of the apparatus. The thrust stand has a natural "home" position which is the pivot's neutral position. When there are no external forces on the thrust stand, the arm should always return to this neutral position. If the thrust stand is not perfectly level, the arm would list to one side, and the resulting bias would be dependent on the weight on the thrust stand and the magnitude of the imbalance. An excellent discussion of the effect of balance on the absolute thrust measurements can be found in Ref. 7. In short, slight imbalances have the effect of altering the effective spring constant, and are a minor effect as long as the spring constant is known, remains consistent throughout the measurement, and the deviation is relatively small. In practice, this requires that the thrust stand be calibrated immediately before and after the measurement. To minimize the off-axis stress on the pivot, the surfaces below and above the pivot must both be level. Shown in the photo are two machinists' bubble levels used to monitor the levelness of the lower surface in the X and Y directions, and a circular level used to balance the upper surface. Motorized actuators (Newport 860) were used to level the thrust stand main breadboard. The actuators were controlled remotely from outside the vacuum chamber, and alignment mirrors were used to view the bubble levels, as there was only one window located at the front of the chamber.

The second factor is vibrational noise. Vibrational noise not only causes the arm to oscillate at its natural frequency, it also causes the optical displacement meter to vibrate and may even cause the thrust stand to become unbalanced, causing the spring constant to drift during a measurement. It is therefore crucial to minimize vibrational noise. The largest source of vibrational noise was the roughing pump. To minimize its contribution, a long (~ 8 ft) foreline was utilized. The pump was set upon several sacks of sand on top of a rolling padded dolly on a thick pad of neoprene, and was placed as far from the experiment as possible. The foreline was also set on a dolly and buried underneath sacks of sand. The thrust stand itself was mounted onto an optical breadboard, which was set on top of another optical breadboard, separated by high-frequency damping springs.

C. Vacuum Chamber

The vacuum chamber is approximately 5' long and 3' in diameter. It has a baseline pressure of approximately $4*10^{-7}$ Torr and is pumped by a roughing pump (Leybold D16B) and two Leybold turbopumps (1650 and 850 lps) for a total pumping speed of 2500 lps.

III. Calibration

The force exerted between the electrodes was experimentally determined using a microbalance (Sartorius CPA 225D). The microbalance has a resolution of 10 µg, or 0.1 µN, but in practice, the balance is accurate to 0.3 – 0.5 µN. When a voltage bias (SRS PS350, PS325) was applied between the electrodes, the lifting force was directly measured. Voltages which supplied forces up to about 100 µN were tested. Measurements of force were made at a number of different electrode separation distances.

The spacing between the electrodes was set using a remote translational stage, accurate to <2 µm. The spacing was set by moving the top electrode towards the bottom electrode until the balance read some fluctuation, indicating the "touch" condition. The translational stage was then moved another few µm, and then reversed until the balance just read the value before the "touch" condition. Then the translational stage was moved to the desired spacing. This procedure minimized errors associated with backlash. The optical displacement meter was included in the setup and verified that the electrode spacing did not change with voltage bias. Both electrodes were electrically isolated from the surroundings. The upper electrode's tilt was adjusted manually using an optical mount. Thin and flexible bare wires (0.1 mm diameter) were used to deliver voltage to the electrodes. The entire setup was encased in a plexiglass box to minimize air currents, and the experiment was carried out on a vibration-damping optical table.

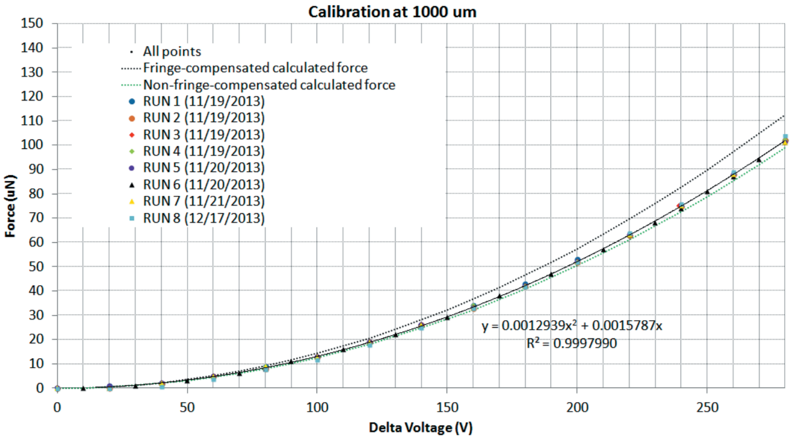

Figure 2. Calibration at electrode spacing = 1000 µm

Calibration curves were generated for electrode spacings from 500 µm to 1500 µm, in 50 µm increments and compared with the fringe uncompensated, parallel plate capacitor (Eq. 2) as well as the fringe-compensated equation given in Ref. 6. All three agreed within a few percent. However, since a thrust stand accuracy of < +/- 1 µm was desired, it is clear that the experimental micro-balance measurements were necessary. The calibration curve for 1000 µm is shown in Fig. 2 as an example.

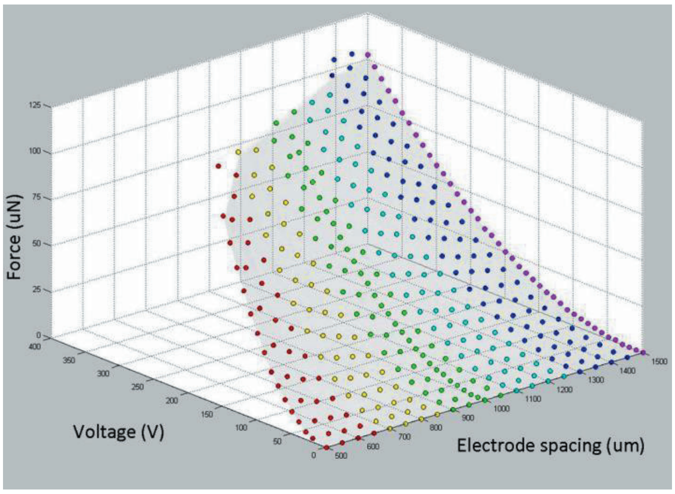

Figure 3. 3D electrostatic calibration plot
The plot enables the interpolation of force with known voltage and electrode spacing.

For each measurement, the "touch" condition was re-established and the spacing was reset. The calibration curves were combined into one 3-D plot in Fig. 3. A Matlab script was generated to interpolate the force given a voltage bias and electrode spacing.

IV. Calculation of Spring Constant, k

Once the microbalance calibration was completed, the results were then used to calculate the flex pivot spring constant. The electrodes were installed on the thrust stand, and using the same power supplies as used for the microbalance procedure, voltage biases were applied. The optical displacement meter recorded the displacement of the thrust stand. A typical calibration is shown in Fig. 4, with close-up. The close-up shows that the natural response of the arm gives a 1/e damping time of approximately 3-5s.

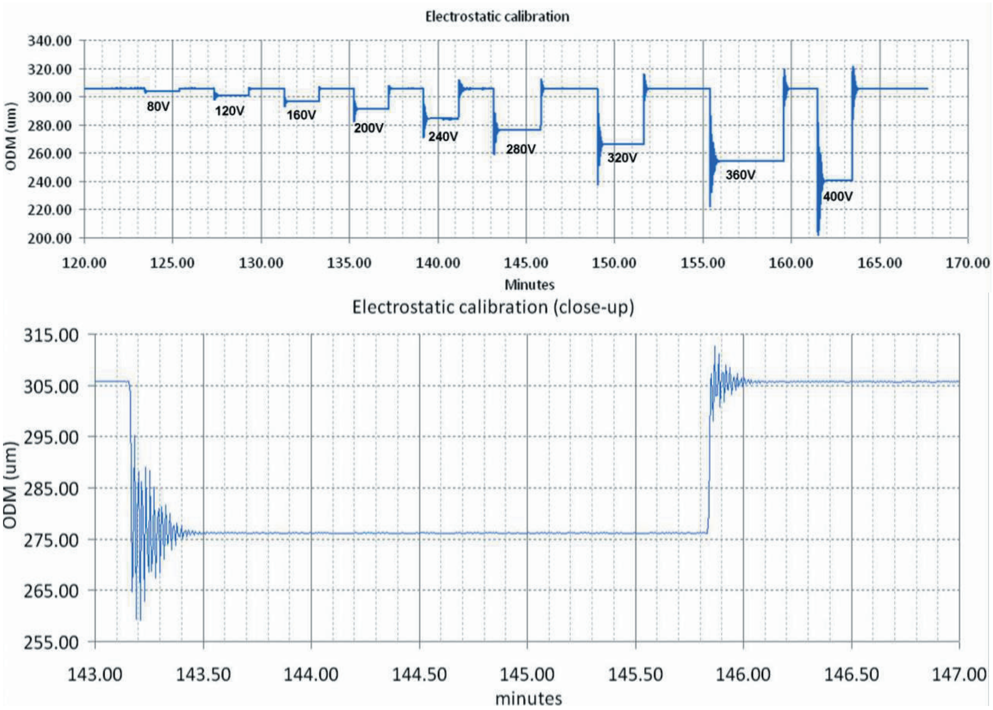

Figure 4. Electrostatic calibration of thrust stand.
*A typical complete calibration is shown in the top plot. Voltages shown are ΔV. A closeup of ΔV=280V is shown in the bottom plot. Chamber pressure, P=3.3*10^{-6} Torr.*

The bias was alternated to minimize the effects of thermal drift over time. To date, 19 calibrations have been completed for a single flex pivot over the course of four months. For each calibration, the thruster stand was re-balanced and the level-ness of the thrust stand and platform was verified. Measurements were taken with the chamber at pressures ranging from 1 atm to 5*10^{-7} Torr, and weight on the thrust stand ranging from 20 to 1100 grams. Each calibration yielded a spring constant, k. The resulting spring constant data are shown in Fig. 5.

It is clear that the spring constant varied about the manufacturer's nominal value, 0.0279 in*lb/deg, thus emphasizing the importance of calibrating the thrust stand immediately before a thrust measurement. The black dotted line represents the thruster force, scaled by its moment arm of 12.7 cm (electrode moment arm = 23 cm) for the last set of data (Dataset 19).

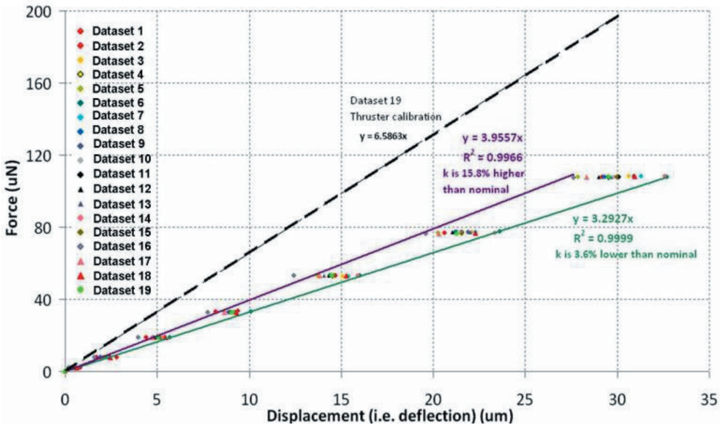

Figure 5. Electrostatic determination of spring constant.

V. Measurements Noise and Resolution

Several sources of noise and/or uncertainty influenced the ultimate precision of the thrust stand. These sources and 1-σ noise contribution are listed in Table 1.

By far, the pumping system noise dominated the measurement resolution limit. The optical displacement meter had a native resolution of 10 nm, which was equivalent to 0.07 µN from Fig. 5. It is difficult to estimate

Table 1. Noise contributions

Noise source	Noise magnitude
Vibration from pumping system	+/- 0.5 µN at sampling rate of 2.5 Hz, with k = 0.279 in*lb/deg
Calibration uncertainties	+/- 0.3 – 0.5 µN
Noise from general lab activities	+/- ~1-10 µN, very short timescale
Thermal drift	+/- ~0.5 µN per hour, long timescale
Noise in optical displacement meter	+/- <0.1 µN at sampling rate of 2.5 Hz
Power supply voltage resolution	+/- 0.1 µN
Electrode spacing	+/- 0.15 µN

uncertainties from the calibration procedure. However, assuming that the voltage bias was 200 +/- 0.2V, a conservative estimate for the SRS350 power supply at an electrode spacing of 1 mm, the resulting force uncertainty would be +/- 0.1 µN. If the electrode spacing were +/- 2 µm, at a electrode bias of 200V and nominal electrode spacing of 1 mm, the resulting force uncertainty would be +/- 0.15 µN. The most significant calibration uncertainty is the uncertainty in the microbalance, 0.3-0.5 µN. In comparison, the noise from general lab activities was mostly sporadic and sudden, and could be seen in the data as a jolt. These include activities such as doors opening and closing, people walking about, earthquakes, etc. These fluctuations would die down quickly (within a few seconds) and were on too short a timescale to impact the measurement. Similarly, thermal drifts were on a long timescale; drifting ~0.5 µN over ~1 hr was typical. The effects of thermal drifts were minimized by not using the chamber lights, and re-zeroing the calibration after each bias was applied. For an actual measurement, thermal drift could be accounted for by re-zeroing often. Another solution is to apply a linear fit to the baseline if the drift is constant over a long period of time. The pumping system (namely the roughing pump) accounted for +/- ~0.05 µm vibration fluctuations, which correspond to about +/- 0.4 µN of force uncertainty based on the nominal spring constant. Important note: the pumping uncertainty was determined from reading the optical displacement meter noise, which was sampled at 2.5 Hz. Since the natural oscillatory damping of the thrust stand arm occurs on the order of a few seconds, it would be reasonable (depending on the nature of the thruster and thrust measurement) to smooth the data by calculating a running average at a slower rate (eg. 1 Hz), thereby lowering the contribution of pump noise. This oscillatory behavior also limits the temporal resolution of the thrust stand so that steady-state measurements are favored. Also, the flex pivot's spring constant directly affects the pump contribution. For example, with a stiffer spring, there would be less vibrational noise, but the overall system resolution with decrease as well. The opposite is also true.

VI. Ongoing and Future Work

Currently, the thrust stand is being used to characterize electrospray thrusters[8-10] which generate thrust in the tens of µN range. The thrust stand test load is limited by the flex pivot. This particular flex pivot has a limit of 38 lbs. However, lighter systems are favored because the lighter the thruster, the easier it is to balance the thrust stand.

Plume diagnostics are being installed in the chamber so that plume characterization measurements can be made in-situ with thrust measurements.

There are several tasks underway to improve the torsional thrust stand. First, we plan to investigate automation of the thrust stand through 2-axis electromagnetic controlled balancing. This would provide the user with the option to balance the thrust stand outside of the vacuum chamber, and is valuable because oftentimes, the thrust stand becomes unbalanced through simply closing the vacuum chamber door and turning on the pumps. Also, we have purchased Nano-Force micro-sensors (Nano-Science, FTS100) which have the capability to measure µN force levels. We would like to investigate ways of incorporating these into the thrust stand. Ideally, these sensors would provide an in-situ duplicate thrust measurement. Reducing vibrational noise continues to be an issue. We plan to investigate ways of further reducing noise, such as upgrading/replacing/relocating the pumping system, or perhaps relocating the experiment to a quieter atmosphere. An additional task could be completion of a trade study into methods of damping the thrust stand's natural oscillations, and how these damping methods would affect temporal resolution. Several candidate methods include viscous liquid damping and simply applying a low-pass filter to the thrust stand data. Similarly, an investigation into noise trade-offs between flex pivot spring constant and thrust measurement resolution would be useful.

VII. Conclusion

A torsional thrust stand has been designed, built, and calibrated which is best suited for steady-state thrust measurements up to approximately 100 µN. This thrust range is ideal for CubeSat propulsion systems and scalable technologies. The upper limit of the thrust stand could easily be raised by extending the range of the micro-balance calibration to higher thrust levels. The resolution of the thrust stand is estimated to be better than +/- 1 µN, and is limited primarily by the roughing pump vibrations. Improvements of the thrust stand facility are in progress, and will include in-situ plume characterization capabilities, improved automation, and further noise reduction.

VIII. Acknowledgments

We would like to thank Byron Zeigler, Kevin Dorman, and Nicholas Drake for their assistance with these experiments. We would also like to acknowledge support from The Aerospace Corporation's Sustained Experimentation and Research for Program Applications program.

IX. References

[1]Yang, Y., Tu, L., Yang, S., Luo, J., "A Torsion Balance for Impulse and Thrust Measurements of Micro-Newton Thrusters," Review of Scientific Instruments, Volume 83, 2012.

[2]Cofer, A., Heister, S., Alexeenko, A., "Improved Design and Characterization of MicroNewton Torsional Balance Thrust Stand," AIAA-2013-3856

[3]Soni, J., Zito, J., Roy, S., "Design of a microNewton Thrust Stand for Low Pressure Characterization of DBD Actuators," AIAA-2013-0755

[4]Merkowitz, S., Maghami, P., Sharma, A., Willis, W., Zakrzwski, C., "A uNewton Thrust-Stand for LISA," Classical and Quantum Gravity, Volume 19, Number 7, 2002 , pp. 1745-1750(6).

[5]Gamero-Castano, M., "A Torsional Balance for the Characterization of MicroNewton Thrusters," Review of Scientific Instruments, Vol. 74, 2003.

[6]Gamero-Castano, M., Hruby, V., "A Torsional Balance that Resolves Sub-micro-Newton Forces," IEPC-01-235

[7]Ziemer, J., "Performance Measurements Using a Sub-Micronewton Resolution Thrust Stand," IEPC-01-238

[8]Lozano, P., Manuel, M., "Ionic Liquid Ion Sources: Characterization of Externally Wetted Emitters," Journal of Colloid and Interface Science, vol. 282, 2005.

[9]Arestie, S., Whitlock, C., Lozano, P., "Ion Electrospray Propulsion System Feasibility Study for Various Satellite Missions and Architectures," AIAA 2013-3877

[10]Masuyama, K., Lozano, P., "Bimodal Propulsion System Using Ionic Liquid Propellant for Pico- and Nano-satellite Applications," AIAA 2013-3962